

MAGNETORQUER-ONLY ATTITUDE CONTROL OF SMALL SATELLITES USING TRAJECTORY OPTIMIZATION

Andrew Gatherer*, Zac Manchester*

This paper presents a magnetorquer-only attitude control technique that utilizes trajectory optimization methods to circumvent the underactuated nature of satellite magnetic field interactions. Given a known orbit and desired attitude state, the method utilizes a nonlinear dynamics model and a fast constrained trajectory optimization solver based on differential dynamic programming to arrive at a nominal torque profile that respects the spacecraft's actuator limitations. This nominal maneuver is then tracked using a time-varying linear-quadratic regulator (LQR). To demonstrate the effectiveness and robustness of the proposed control technique, closed-loop Monte-Carlo simulations are performed from a variety of orbits and initial conditions. Our method is shown to significantly outperform previous magnetorquer-only control schemes by offering convergence from large initial errors and fast slew rates that exploit the full performance capabilities of the actuators. Computational complexity of the method and future implementation in flight software onboard a CubeSat are also discussed.

INTRODUCTION

Due to the ever-increasing scope of small satellite missions, there is now significant demand for precise attitude determination and control capabilities onboard CubeSats. Often, traditional attitude control methods like reaction wheels and thrusters are prohibitively expensive in terms of mass, volume, power, and cost for CubeSat missions, necessitating alternative approaches.

Interactions between magnetic torque coils and the Earth's magnetic field have been used for decades on board satellites to offload momentum from reaction wheels. However, magnetorquers are inherently underactuated, complicating their application to full three-axis pointing. Beginning in 1976 with Stickler and Alfriend,¹ magnetorquers were suggested as a replacement for reaction wheels as a form of momentum bias in satellites. Many authors, including Martel and Piaski² and Arduinni and Baiocco,³ have illustrated the use of magnetorquers in concert with gravity gradient systems, which were validated on orbit during the Orsted mission.⁴ In order to make a truly self-sufficient magnetorquer control system, some authors, such as Lovera,⁵ Pittelkau,⁶ and Psiaki,⁷ have capitalized on the near-periodic nature of the Earth's magnetic field. Magnetorquer-only attitude control has been tested on orbit by Psiaki⁸ and Wisniewski⁴ using a linearized dynamics model with partial success.

In contrast to these previous approaches, our method does not linearize the satellite attitude dynamics, which allows it to handle large initial errors and fast slewing maneuvers that exploit the full actuator capabilities of the spacecraft. Additionally, a more complex magnetic field model is implemented for better utilization of the Earth's intricate magnetic environment. Our method is more

*Department of Aeronautics and Astronautics, Stanford University, 496 Lomita Mall, Stanford, CA 94305.

computationally expensive than prior approaches, but is well within the capabilities of the modern microcontrollers that are typically flown on CubeSats. Finally, it is important to emphasize that this algorithm can be used completely independently of traditional reaction wheels, thrusters, or gravity gradient systems, greatly increasing capabilities of resource-constrained small satellites.

The paper proceeds as follows: the next section introduces the magnetic field model and assumptions used in our approach. The Controllability section then develops a method for estimating maneuver duration. Then, the orbit and attitude dynamics models used for both simulation and trajectory optimization are presented. The Trajectory Optimization section details the trajectory optimization problem formulation and provides a procedure to efficiently handle quaternion differentiation. The LQR Tracking Controller section presents a method used to track the trajectory online with special consideration for the quaternion part of the state vector. The Simulations section illustrates the utility of the method on different satellite sizes and orbits. Additionally, a comparison to previous work is given. Finally, we outline our conclusions.

MAGNETIC FIELD MODEL

Unlike the low-order periodic assumptions required for the periodic LQR methods of Psiaki et al.,⁷ we use a high-fidelity magnetic field model. Although it is computationally expensive to incorporate a more accurate magnetic field, the greater variation in field direction facilitates improved control authority over shorter time scales, especially in equatorial or near-equatorial orbits.

A spherical harmonic expansion of degree and order three is used to model the magnetic field (Figure 1), with coefficients specified by the 12th generation International Geomagnetic Reference Field² (IGRF):

$$B(r, \theta, \phi, t) = -\nabla V(r, \theta, \phi, t), \quad (1)$$

$$V(r, \theta, \phi, t) = a \sum_{n=1}^M \sum_{m=1}^n \left(\frac{a}{r}\right)^{n+1} [g_n^m(t) \cos(m\phi) + h_n^m(t) \sin(m\phi) P_n^m(\cos \theta)], \quad (2)$$

where B is the magnetic field vector and V is the magnetic scalar potential. We found that truncating the IGRF model at this level of accuracy provided computational benefits without imposing significant inaccuracies on the trajectory optimization results. By using a higher-order model, our method is able to reach arbitrary orientations even in equatorial orbits where a method using a dipole model typically fails.

DYNAMICS MODEL

Our method requires the ability to simulate both the orbital and attitude dynamics of the spacecraft. The satellite orbit is propagated using a gravitational field with the J_2 oblateness term,

$$f_{grav} = -\frac{\mu r}{\|r\|^3} + \begin{bmatrix} \frac{J_2 r_1}{\|r\|^7} (6r_3 - 1.5(r_1^2 + r_2^2)) \\ \frac{J_2 r_2}{\|r\|^7} (6r_3 - 1.5(r_1^2 + r_2^2)) \\ \frac{J_2 r_3}{\|r\|^7} (3r_3 - 4.5(r_1^2 + r_2^2)) \end{bmatrix}, \quad (3)$$

where r is the position of the satellite, μ is the standard gravitational parameter for Earth, and J_2 is a constant used in calculating the disturbance from Earth oblateness. Due to the inherent uncertainty in the magnetic field model and the short time scales over which attitude maneuvers occur, other perturbations such as drag, solar radiation pressure, and higher order gravitational terms are not significant.

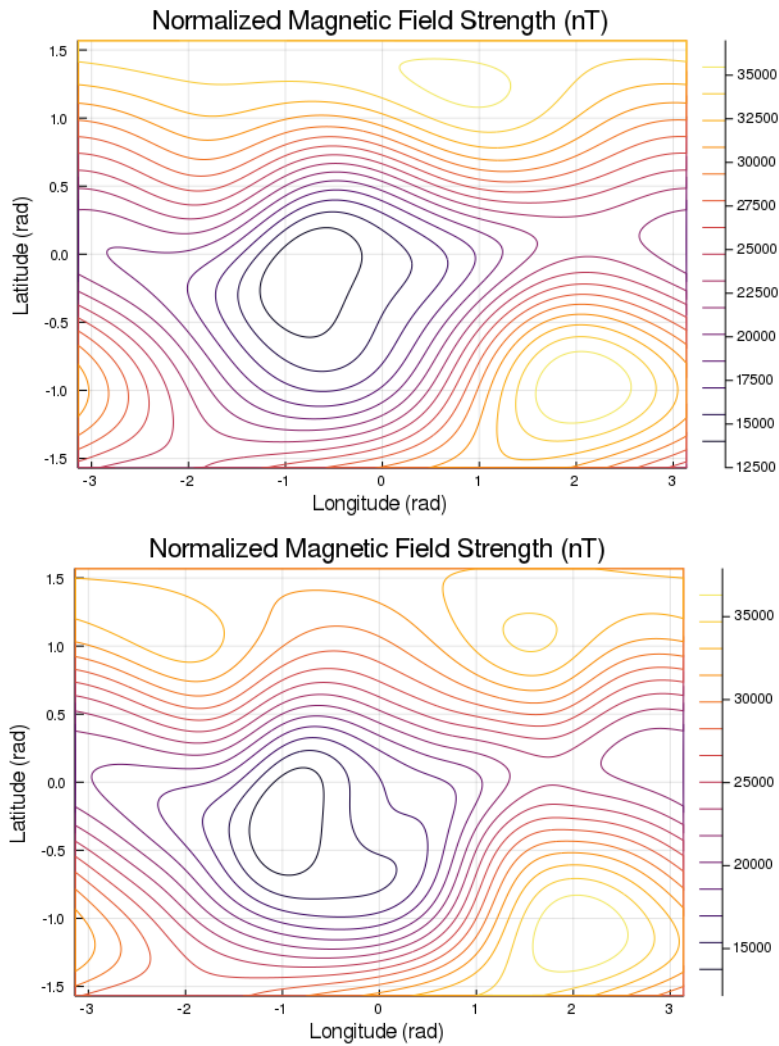


Figure 1. Comparison between 3rd order magnetic field (top) and full IGRF model (bottom).

The attitude dynamics are modeled using Euler's equation,

$$J\dot{\omega} + \omega \times J\omega + B(r) \times u = 0, \quad (4)$$

where J is the spacecraft's moment of inertia, ω is the angular velocity, B is the local magnetic field vector, and u is the magnetic moment applied by the torque coils.

We use unit quaternions to parameterize the attitude of the spacecraft, with kinematics given by,

$$\dot{q} = \frac{1}{2} \begin{bmatrix} -q_2 & -q_3 & -q_4 \\ q_1 & -q_4 & q_3 \\ q_3 & q_1 & -q_2 \\ -q_3 & q_2 & q_1 \end{bmatrix} \omega = \frac{1}{2} W(q)\omega \quad (5)$$

The standard 4th order Runge-Kutta method is employed to integrate the equations of motion. Gravity gradient torques are assumed to be negligible, but future work might consider those affects as well as atmospheric drag torques.

CONTROLLABILITY

Magnetic field behavior varies widely depending on the orbital elements of the spacecraft, which makes determining the length of time required to perform an attitude maneuver difficult. Since free-final-time or infinite-horizon trajectory optimization problems are computationally expensive to perform, an alternative method of determining a maneuver length was devised. A necessary condition for full controllability of the system is that the actuators must be able to produce torques about all three coordinate axes (in the inertial reference frame) over the course of the trajectory. We therefore define the following controllability Grammian \mathcal{C} ,

$$\mathcal{C}(t_0, t_f) = \int_{t_0}^{t_f} B^\times(\tau)B^\times(\tau) d\tau, \quad (6)$$

where B^\times is the skew-symmetric matrix associated with the cross product of B :

$$B^\times = \begin{bmatrix} 0 & -B_3 & B_2 \\ B_3 & 0 & -B_1 \\ -B_2 & B_1 & 0 \end{bmatrix}. \quad (7)$$

Full three-axis controllability is achieved if \mathcal{C} has rank 3. Since the matrix B^\times always has rank 2, \mathcal{C} can only achieve full rank if the magnetic field vector changes direction along the trajectory. We use the condition number of \mathcal{C} , defined as the ratio of its maximum and minimum singular values, as a qualitative metric of its invertability. Equation (7) is integrated forward in time until the condition number reaches a chosen cutoff value. That cutoff time is then used as the fixed final time for the maneuver in the trajectory optimizer. This heuristic procedure ensures that sufficient time is allotted for trajectories in near-equatorial orbits, where the magnetic field is slowly varying, while also allowing shorter maneuver times in higher-inclination orbits.

TRAJECTORY OPTIMIZATION

We formulate the attitude control problem as the following optimization problem,

$$\begin{aligned}
& \underset{x_{1:N}, u_{0:N-1}}{\text{minimize}} && \ell_f(x_N) + \sum_{k=0}^{N-1} \ell_k(x_k, u_k) \\
& \text{subject to} && x_{k+1} = f(x_k, u_k), \quad k = 0, \dots, N-1,
\end{aligned} \tag{8}$$

where ℓ_k and ℓ_N are stage and terminal cost functions, $x_k = \begin{bmatrix} \omega_k \\ q_k \end{bmatrix}$ is the state vector, u_k is the control input, $f(x, u)$ is the attitude dynamics model defined in the previous section, and k is the time-step index.

Since the quaternion is a non-minimal attitude representation that always has unit norm, the simple quadratic cost functions frequently used in optimal control problems are inappropriate. Instead, a three-parameter error representation is penalized. A 6×7 Jacobian matrix, $G(q)$, that maps a quaternion to this three-parameter representation is used to define the following cost function:

$$\ell_f(x_N) = \frac{1}{2} x_N^T G^T(q_d) Q_N G(q_d) x_N \tag{9}$$

$$\ell_k(x_k, u_k) = \frac{1}{2} x_k^T G^T(q_c) Q G(q_c) x_k + \frac{1}{2} u_k^T R u_k, \tag{10}$$

where q_d is the desired final attitude quaternion and $G(q)$ is defined as follows:

$$G(q) = \begin{bmatrix} 1 & 0 & 0 & 0 & 0 & 0 & 0 \\ 0 & 1 & 0 & 0 & 0 & 0 & 0 \\ 0 & 0 & 1 & 0 & 0 & 0 & 0 \\ 0 & 0 & 0 & -q_2 & q_1 & q_4 & -q_3 \\ 0 & 0 & 0 & -q_3 & -q_4 & q_1 & q_2 \\ 0 & 0 & 0 & -q_4 & q_3 & -q_2 & q_1 \end{bmatrix}. \tag{11}$$

We solve problem (8) using the ALTRO solver,⁹ which is based on iterative LQR with an augmented Lagrangian method for handling constraints. ALTRO is fast and has modest computing requirements, making it suitable for embedded implementation onboard small satellites. Note, also, that all evaluations of the magnetic field and associated Jacobian matrices can be pre-computed, as they are only functions of the satellite orbit, and do not need to be re-calculated as part of the trajectory optimization solution process.

LQR TRACKING CONTROLLER

After optimizing a nominal state and input trajectory, a time-varying LQR (TVLQR) feedback controller⁷ is used to track the nominal trajectory online. Special consideration must be made for the quaternion in the state vector. First, the dynamics listed in equations (4)–(5) are linearized:

$$A_k = \left. \frac{\partial f}{\partial x} \right|_{x_k} \quad B_k = \left. \frac{\partial f}{\partial u} \right|_{x_k}. \tag{12}$$

As with the cost functions in the iterative LQR solver, a coordinate transformation must be applied to the linearized dynamics to convert the quaternions to a three-parameter error representations using the $G(q)$ Jacobian matrix:

$$\tilde{A}_k = G(q_k) A_k G(q_k)^T \quad \tilde{B}_k = G(q_k) B_k. \tag{13}$$

The standard algebraic Ricatti equation is used to calculate a time-varying LQR tracking controller:

$$S_N = Q_N \quad (14)$$

$$K_k = (R + \tilde{B}_k^T S_{k+1} \tilde{B}_k)^{-1} \tilde{B}_k^T S_{k+1} \tilde{A}_k \quad (15)$$

$$S_k = Q + K_k^T R K_k + (\tilde{A}_k - \tilde{B}_k K_k)^{-1} S_{k+1} (\tilde{A}_k - \tilde{B}_k K_k). \quad (16)$$

The control law is then,

$$u_k = \bar{u}_k - K_k \delta x_k, \quad (17)$$

where \bar{u}_k is the nominal control input generated by the trajectory optimizer and the state tracking error is,

$$\delta x_k = \begin{bmatrix} \omega_k - \bar{\omega}_k \\ 2\phi \end{bmatrix}, \quad (18)$$

where $\bar{\omega}_k$ is the nominal angular velocity from the optimized trajectory and ϕ is the three-parameter attitude tracking error represented as Modified Rodrigues parameters,¹⁰

$$\phi = \frac{e_{2:4}}{1 + e_1}, \quad (19)$$

where e_1 and $e_{2:4}$ are the scalar and vector parts of the quaternion error:

$$\begin{bmatrix} e_1 \\ e_{2:4} \end{bmatrix} = \begin{bmatrix} \bar{q}_1 q_1 + \bar{q}_{2:4}^T q_{2:4} \\ \bar{q}_1 q_{2:4} - q_1 \bar{q}_{2:4} - \bar{q}_{2:4} \times q_{2:4} \end{bmatrix}. \quad (20)$$

SIMULATIONS

Two different satellites were considered in the simulation: 1U and 3U CubeSats. Both satellites were tasked to slew 180° as an example attitude maneuver. In all simulations, the satellites were initialized with zero angular velocity. Zero-mean Gaussian noise was applied to the state and the magnetic field as detailed in Table 1.

Table 1. Satellite Noise Statistics

Sensor	Variance
Rotation Rate (deg s ⁻¹)	0.38
Attitude (deg)	1.0
Magnetometer (T)	1.0e-5

CubeSat Properties

The satellite properties for both the 1U and 3U cases are tabulated below. Both satellites were assumed to have uniform mass distribution and products of inertia equal to zero.

Table 2. 1U CubeSat Properties

Property	Value
Mass (kg)	0.75
$J_{xx} = J_{yy} = J_{zz}$ (kg m ²)	0.00125
Maximum Magnetic Moment (A m ²)	0.19

Table 3. 3U CubeSat Properties

Property	Value
Mass (kg)	3.5
J_{xx} (kg m ²)	0.005256
$J_{yy} = J_{zz}$ (kg m ²)	0.04939
Maximum Magnetic Moment (x) (A m ²)	0.19
Maximum Magnetic Moment (y = z) (A m ²)	0.57

1U Pointing

In order to validate the performance of the magnetorquer-only control system, 180° slews were demonstrated on a 1U CubeSat. The CubeSat in this simulation was initialized in an ISS orbit beginning at the ascending node. The attitude, rotation rate, and control input of this maneuver are shown in Figure 2.

3U Pointing

The ability of the control system to slew a comparatively larger 3U CubeSat was also demonstrated. Again, this case was initialized in an ISS orbit beginning at the ascending node. Importantly, the CubeSat was rotated about its major axis of inertia, maximizing the amount of time needed to slew. Again, the attitude, rotation rate, and control input of this maneuver are shown in Figure 3.

1U Monte Carlo

Since the performance of the controller is highly dependent on the changing magnetic field, corner cases are a significant concern. To ensure that there were no orbits in which the trajectory optimization method failed, 100 different circular orbits with altitudes of 400 km were tested in three different common CubeSat inclinations, polar, sun-synchronous, and ISS (51.5°). The right ascension and mean anomaly of the starting position were all randomized.

Figures 4, 5, and 6 show histograms of the 100 simulations for each orbit. The runs with the longest slew times were compared against their magnetic fields, and a general correlation was found between slew time and magnetic field variation. The more that the magnetic field vector changed over the course of the simulation, the faster the satellite was able to slew its attitude, as expected. Most importantly, the algorithm exhibited no failure cases and took at most a few minutes to execute the desired slew.

Comparison

We compared our algorithm against the previously formulated "No Wheel" control.^{7,11} The "No Wheel" control system was derived by examining the required torque to slew the satellite to the desired state. This torque was then converted into a feasible magnetic moment through a cross product manipulation with the measured magnetic field,

$$T_{required} = -(C_1\bar{\omega} + C_1J^{-1}\bar{q}), \quad (21)$$

$$m_{feasible} = \frac{B_{measured} \times T_{required}}{|B_{measured}|^2}, \quad (22)$$

where $B_{measured}$ is the measured magnetic field vector in the body frame, $\bar{\omega}$ is the rotation rate of the body frame axes with respect to the trajectory frame, \bar{q} is the vector component of the attitude quaternion between the body frame and the trajectory frame, and C_1 and C_2 are chosen constants.

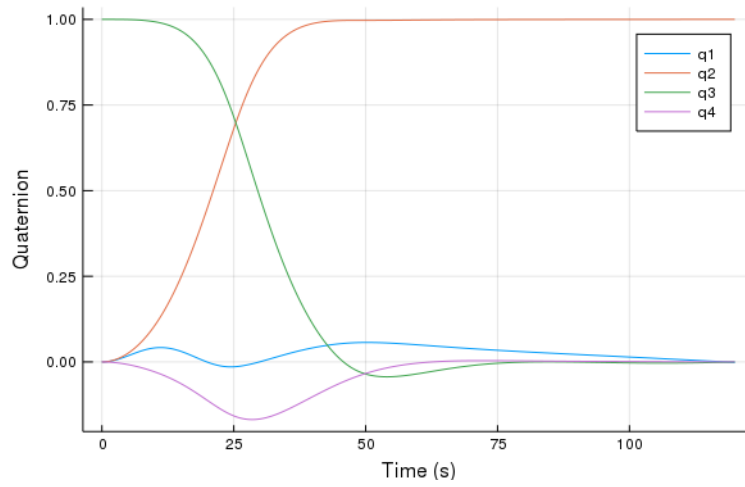
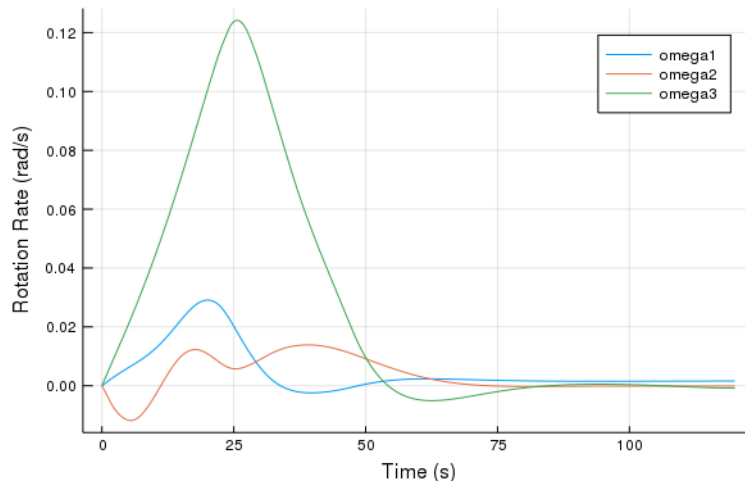
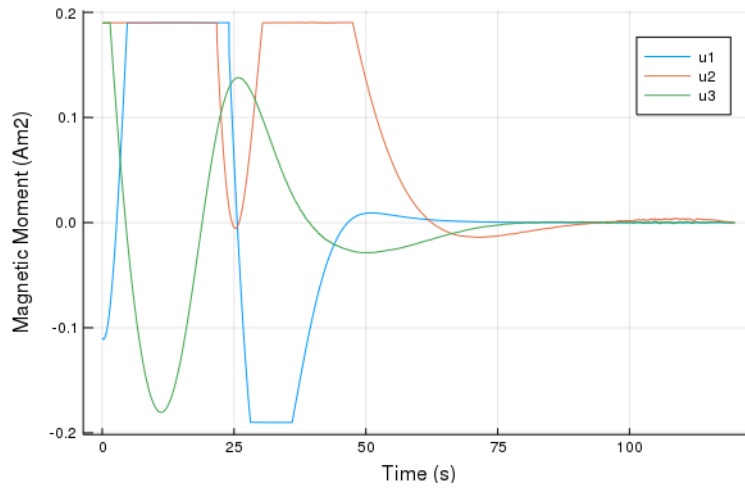


Figure 2. 1U Simulation Results

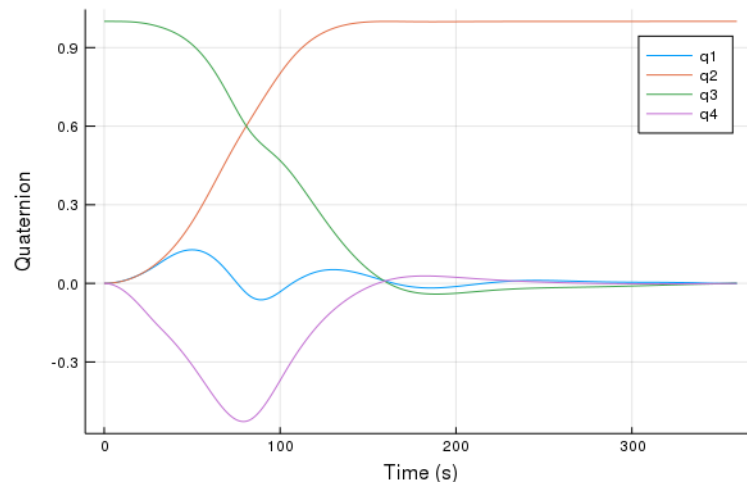
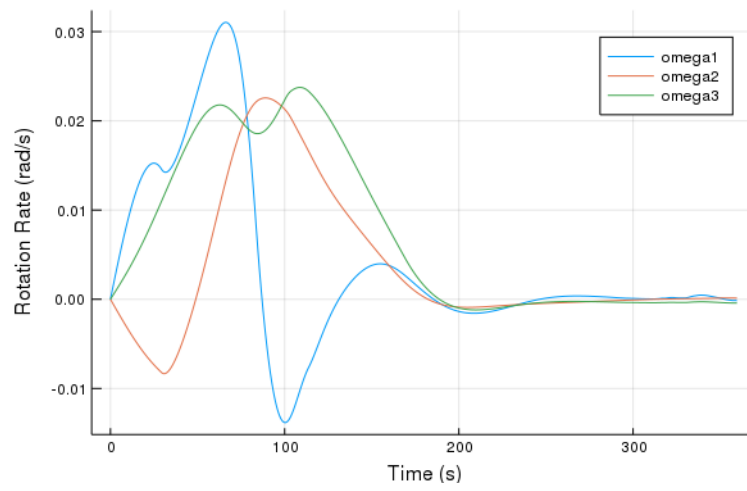
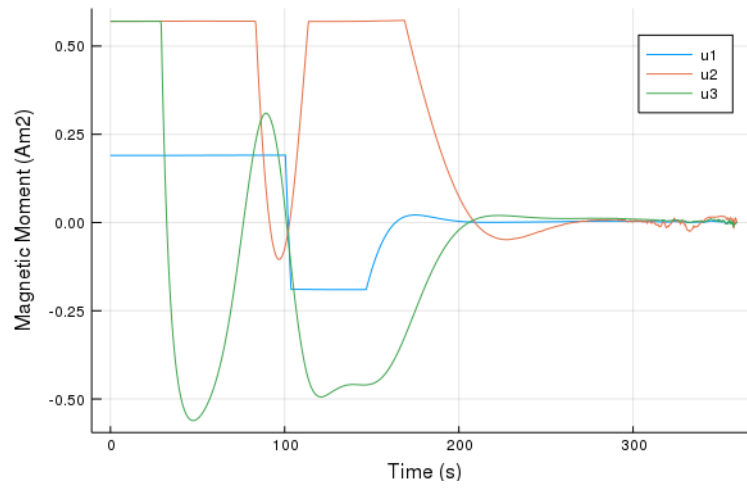


Figure 3. 3U Simulation Results

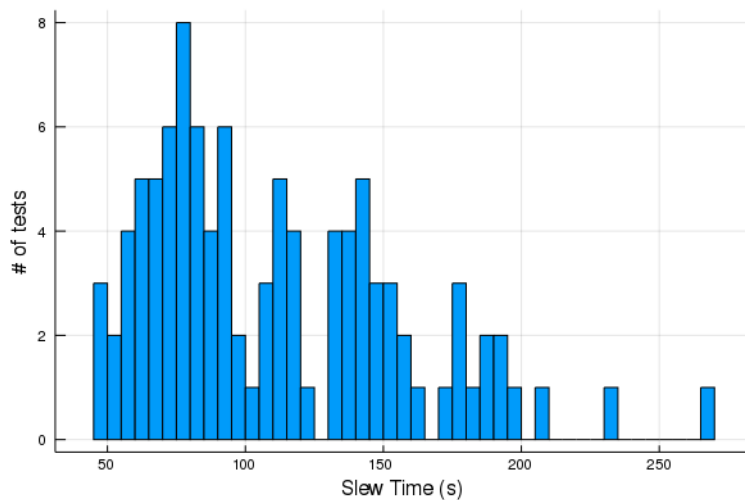


Figure 4. Polar Monte-Carlo Simulation

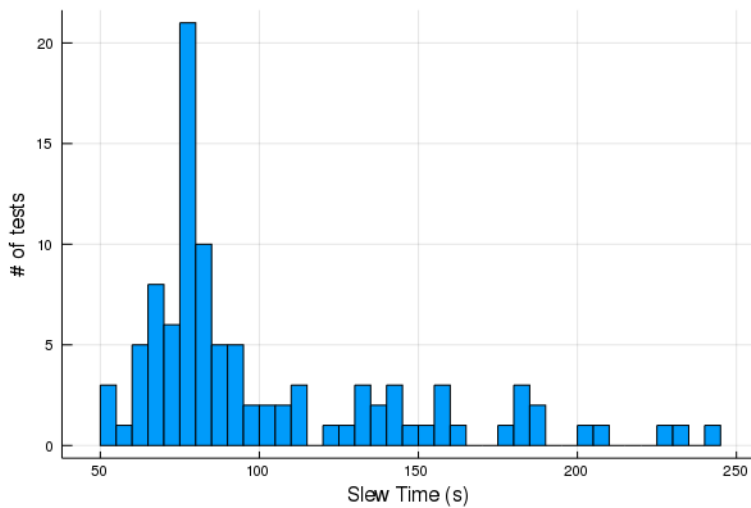


Figure 5. SSO Orbit Monte-Carlo Simulation

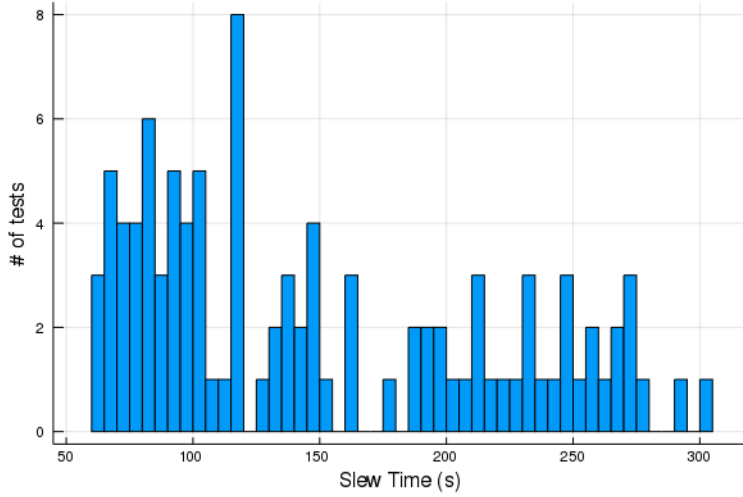


Figure 6. ISS Orbit Monte-Carlo Simulation

The "No-Wheel" control law was simulated in randomly selected orbits with the same 1U CubeSat parameters described in the previous section. The control law showed reasonable convergence for small attitude errors of up to 10° when the constants could be tailored to the magnetic field strength along the orbit. Even then, the control system showed significant oscillatory behavior, especially over satellite orbits where the magnetic field deviated significantly from a dipole model. For initial errors greater than 10° , this control method failed to converge in our tests. Additionally, this method results divergence if the satellite has a large initial rotation rate. The results of a simulation with 90° initial error are shown in Figure 8.

The Asymptotic Periodic Linear Quadratic Regulator (APLQR)¹¹ was also tested. In this method, the satellite dynamics are linearized, and the control law is based on the known magnetic field and the solution of a time-invariant Riccati equation:

$$u(t) = -R^{-1}B^T(t)P_{ss}x(t) \quad (23)$$

where $u(t)$ is the control input to the magnetorquers, $B(t)$ is a function of the magnetic field, $x(t) = [\phi \ \theta \ \psi \ \omega_{sc/ll1} \ \omega_{sc/ll2} \ \omega_{sc/ll3}]^T$, and P_{ss} is found through solving Equation (24).

$$0 = -P_{ss}A - A^T P_{ss} - Q + P_{ss}(\epsilon\tilde{B}_0)(\epsilon\tilde{B}_0)^T P_{ss} \quad (24)$$

The APLQR control law found using a simplified periodic assumption of the magnetic field was simulated in the higher-fidelity IGRF model on a satellite with 1U CubeSat parameters. The control law was found to converge to within 5° of the desired attitude from initial errors as high as 30° for orbits with high inclinations, but unstable behavior was encountered in orbits with inclinations less than 60° . For lower inclination orbits, the control effectiveness matrix utilized to calculate the P_{ss} matrix based on the first-order Earth magnetic field is poorly conditioned, rendering stability over all axes impossible. Additionally, the APLQR controller could not account for initial attitude errors beyond 30° .

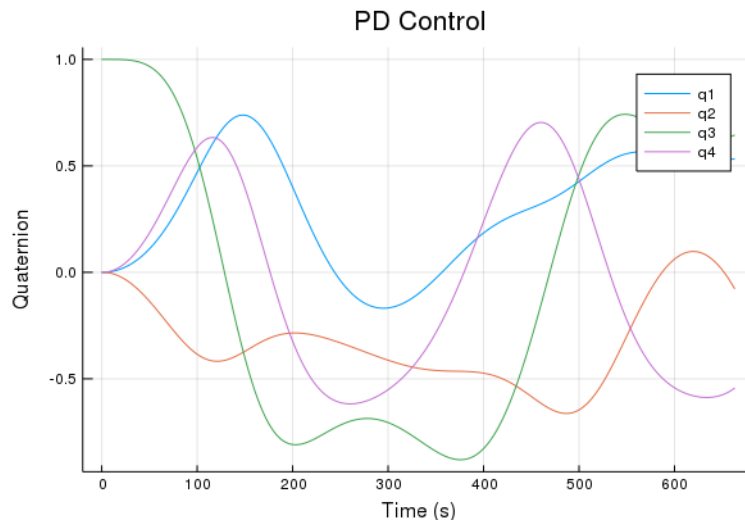


Figure 7. Proportional-Derivative Control

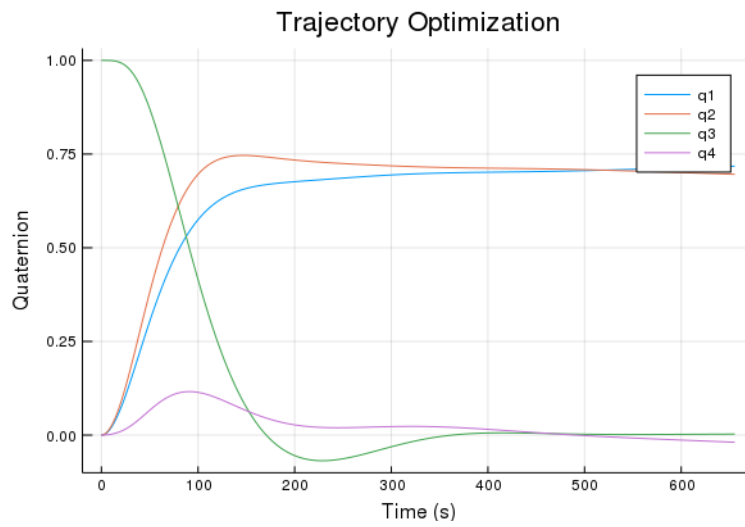


Figure 8. Trajectory Optimization Control

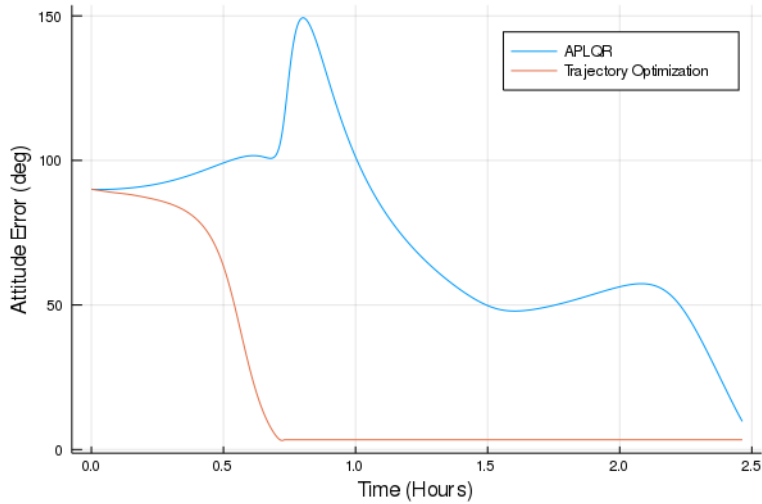


Figure 9. APLQR Comparison

Even in the best case conditions, the trajectory optimization algorithm presented in this paper significantly outperformed the APLQR control law. APLQR requires many orbits to converge, while our method is able to converge in minutes, as shown in Figure 9.

CONCLUSIONS

We have proposed a novel attitude control technique for small satellites that uses only magnetic torque coils and relies on onboard solution of a trajectory optimization problem to produce a nominal trajectory, which is then tracked with a time-varying LQR controller. The control technique was simulated on both 1U and 3U CubeSats in many different orbits, demonstrating its effectiveness under a wide range of conditions.

Magnetorquer-only control, though underactuated, provides significant promise for small satellites. Torque coils scale favorably in terms of size, mass, and power, and magnetorquer-based control also eliminates the jitter associated with reaction wheels. By considering higher order magnetic fields rather than a simplified dipole models, magnetic-field-based control is more effective due to significant local changes in the magnetic field vector. While our method has significant computational overhead, it is well within the capabilities of the modern microcontrollers currently being flown onboard CubeSats.

ACKNOWLEDGEMENTS

The authors would like to thank Brian Jackson and Taylor Howell for assistance with the ALTRO trajectory optimization software.

NOMENCLATURE

ω Angular Velocity

ρ Density

τ	Torque
τ_{mag}	Torque from Magnetic Interaction
B	Magnetic Field
f	Acceleration
m	Magnetic Moment
v	Velocity
M	Specific Gravitational Parameter
h	Height
I	Current
J	Moment of Inertia
q	Quaternion
r	Radius

REFERENCES

- [1] A. C. Stickler and K. Alfriend, "Elementary Magnetic Attitude Control System," *Journal of Spacecraft and Rockets*, Vol. 13, May 1976, pp. 282–287, 10.2514/3.57089.
- [2] F. Martel, P. Pal, and M. Psiaki, "Active Magnetic Control System for Gravity Gradient Stabilized Spacecraft," p. 18.
- [3] C. Arduini and P. Baiocco, "Active Magnetic Damping Attitude Control for Gravity Gradient Stabilized Spacecraft," *Journal of Guidance, Control, and Dynamics*, Vol. 20, Jan. 1997, pp. 117–122, 10.2514/2.4003.
- [4] R. Wisniewski, "Linear Time-Varying Approach to Satellite Attitude Control Using Only Electromagnetic Actuation," *Journal of Guidance, Control, and Dynamics*, Vol. 23, July 2000, pp. 640–647, 10.2514/2.4609.
- [5] M. Lovera, E. De Marchi, and S. Bittanti, "Periodic Attitude Control Techniques for Small Satellites with Magnetic Actuators," *IEEE Transactions on Control Systems Technology*, Vol. 10, No. 1, Jan./2002, pp. 90–95, 10.1109/87.974341.
- [6] M. E. Pittelkau, "Optimal Periodic Control for Spacecraft Pointing and Attitude Determination," *Journal of Guidance, Control, and Dynamics*, Vol. 16, Nov. 1993, pp. 1078–1084, 10.2514/3.21130.
- [7] M. L. Psiaki, "Magnetic Torquer Attitude Control via Asymptotic Periodic Linear Quadratic Regulation," *Journal of Guidance, Control, and Dynamics*, Vol. 24, Mar. 2001, pp. 386–394, 10.2514/2.4723.
- [8] M. Guelman, R. Waller, A. Shiryaev, and M. Psiaki, "Design and Testing of Magnetic Controllers for Satellite Stabilization," *Acta Astronautica*, Vol. 56, Jan. 2005, pp. 231–239, 10.1016/j.actaastro.2004.09.028.
- [9] T. A. Howell, B. E. Jackson, and Z. Manchester, "ALTRO: A Fast Solver for Constrained Trajectory Optimization," *IROS 2019*, Feb. 2019. In Review.
- [10] H. Schaub and J. Junkins, *Analytical Mechanics of Space Systems*. AIAA Education Series, Reston, VA: AIAA, 2 ed., 2009.
- [11] M. L. Psiaki, "Backward-Smoothing Extended Kalman Filter," *Journal of Guidance, Control, and Dynamics*, Vol. 28, Sept. 2005, pp. 885–894, 10.2514/1.12108.